Supporting Information

De Ceunynck et al. 10.1073/pnas.1718600115

SI Materials and Methods

Materials and Reagents. Parmodulins were either synthesized at the Broad Institute or purchased from Axon Medchem or Tocris Bioscience and used in 0.1% BSA. TNF-α was obtained from EMD Millipore (LY294002); wortmannin from Selleckchem; gallein and Akt inhibitor (GSK69063) from Tocris Bioscience; staurosporine and PAR4-agonist (AYPGKF) from Sigma Aldrich; human APC and thrombin from Haematological Technologies; and recombinant angiopoietin-1, soluble CD-14 (sCD14), LBP, and recombinant VEGF 165 protein from R&D systems. Cleaved caspase-3 antibody (Asp175), DRAQ5, mouse anti-AKT, rabbit anti-pAKT (Ser473), rabbit anti-pAkt (Thr308), rabbit anti-actin, and rabbit anti-GAPDH antibodies were purchased from Cell Signaling Technologies; rabbit anti-pPI3K p85 (Tyr607) antibody from Abcam; mouse anti-PI3K, mouse anti-human PAR1 antibody (ATAP2), and rabbit anti-human stanniocalcin-1 antibodies from Santa Cruz; and HRP-labeled anti-mouse and anti-rabbit secondary antibodies from Jackson ImmunoResearch Laboratories. LPS from *E. coli* serotype 0111:B4 was obtained from Sigma Aldrich. All other chemicals were of the highest purity grade available commercially.

Coagulation Assays. Human pooled plasma ($n \geq 4$ donors) was incubated with vehicle, APC, or parmodulin 2 at indicated concentrations for 15 min at 37 °C. Following incubation, PT, and aPTT were measured using the Neoplastin Cl Plus and PTT A kits (Diagnostica Stago) according to the manufacturer's instructions. Time until clotting was measured in seconds. Data are represented as the ratio of sample/control plasma.

Platelet Aggregation. Mouse and human washed platelets were isolated, as described previously (1, 2). Washed platelets were diluted to a final concentration of 200,000–250,000 platelets/μL, and platelet aggregation was initiated with PAR4 agonist or thrombin and measured using a ChronoLog 680 aggregometer. At the beginning of each experiment, an agonist dose-curve was run to determine the lowest agonist concentration required for aggregation.

Endothelial Cell Culture. Pooled HUVECs (Lonza) were cultured on gelatin (Stemcell Technologies)-coated flasks and used to a maximum passage number of 6.

Transfection of siRNA and Gene Expression Analysis. Transfections were performed as described previously (3). Validated siRNA for PAR1 (catalog #S4924), STC1 (catalog #S13551), and control siRNA (catalog #4390843) were purchased from ThermoFisher Scientific. Corresponding TaqMan gene expression assay probes (ID Hs00169258_m1 for PAR1; ID Hs00174970_m1 for STC1) were used to confirm reduction of gene expression by qRT-PCR as directed by the manufacturer (ThermoFisher Scientific).

Gene Expression Profiling. HUVECs were treated with vehicle or PM2 for 4 h prior to exposure to buffer or TNF-α (10 ng/ml) for an additional 4 h. Cells were harvested, resuspended in RNAlater (ThermoFisher Scientific), and stored at 4 °C until isolation of total RNA by a PureLink RNA mini kit (ThermoFisher Scientific). Gene expression profiles were obtained using the gene profiling array cGMP U133 P2 (Affymetrix). Procedures were completed at the Microarray Core Facility of Dana-Farber Cancer Institute. Data analysis was performed using the Affymetrix Transcriptome analysis console. Positive hits were confirmed using qRT-PCR analysis as described.

NF-κB Reporter Assay. Changes in the activity of the NF-κB–signaling pathway were evaluated using the Cignal GFP NF-κB pathway reporter assay (Qiagen). HUVECs (60% confluency) were transfected with 100 ng of GFP reporter plasmid, negative control plasmid, or positive control GFP plasmid as provided by the manufacturer. After 24 h, transfection medium was replaced by growth medium. Cells were assayed 48–72 h after transfection when full confluency was reached.

Mice. C57BL/6J mice (male; 8–12 wk) were obtained from The Jackson Laboratory. Animal care and experimental procedures were performed in accordance with and under the approval of the Beth Israel Deaconess Medical Center Institutional Animal Care and Use Committee. Mice were anesthetized with i.p. injection of a ketamine (125 mg/kg) and xylazine (12.5 mg/kg) mixture in sterile saline. Anesthesia was maintained with pentobarbital (5 mg/kg) through a jugular vein cannula.

Histology. Paraffin embedding, sectioning, and staining of mouse aorta was performed at the Histology and Microscopy Core of Beth Israel Deaconess Medical Center. Following antigen retrieval in 10 mM sodium citrate (pH 6), sections were incubated with 1 mg/mL sodium borohdyride (ICN Chemicals) for 5 min at room temperature. Blocking was performed for 1 h at room temperature (RT) with 5% normal donkey serum (Jackson ImmunoResearch Laboratories) followed by incubation with rabbit anti-STC1 (1:100, catalog # sc-30183; Santa Cruz Biotechnology) overnight at 4 °C. Alexa 647-conjugated donkey anti-rabbit secondary antibodies (1:200; Jackson ImmunoResearch Laboratories) were used for detection. Slides were mounted with Prolong Gold anti-fade mounting media (ThermoFisher Scientific), and images were captured as described above.

Endothelial Activation in Vivo. Following cannulation of the jugular vein, 10 mg/kg parmodulin 2 in sterile saline containing 5% Tween-80 was infused into the animal i.v. 3 h before saline or LPS (10 mg/kg) administration i.p. An additional bolus injection of either saline or parmodulin 2 was given at the time of saline or LPS exposure. After 3 h, blood was collected on 3.2% citrate and spun down at 2,800 × *g* for 15 min to obtain platelet-poor plasma. Soluble E-selectin levels were measured in plasma using the mouse E-selectin Quantikine ELISA kit (R&D Systems) according to the manufacturer's instructions. VWF levels were measured using an in-house ELISA as previously described (3).

Leukocyte Rolling. Following jugular vein cannulation, animals were treated i.v. with 10 mg/kg parmodulin 2 in sterile saline containing 5% Tween-80 for 3 h before exteriorization of the cremaster. Observations were made with an intravital microscope (Olympus) with a saline immersion objective (SW 40, 0.75 N.A.). Cremasteric venules were observed and recorded using a Sony analog camera for 60 s. Data were collected for 1 h following the first scrotal incision. At the end of the experiment, total blood was collected via cardiac puncture and diluted 1:10 with sodium citrate, and total leukocyte concentration was measured by veterinary Hemavet (Drew Scientific). Rolling leukocytes were counted for 30 s as they crossed a centerline and leukocytes that were stationary for >30 s were excluded. The erythrocyte centerline velocity [V_v (μm/s)] in recorded microvessels was measured via injection of dragon green 0.52-μm polystyrene microspheres (Bangs Laboratories) that were diluted 1:20 in saline and injected via jugular cannulus. The velocity of each sphere for six to eight individual spheres was measured using Slidebook 5.5. The measurements were averaged, and

vessels with >10% error were excluded from further analysis. In addition, the mean vessel diameter [D_v (μm)] was measured using Slidebook and used to determine area of the vessel [A_v (μm^2)]. Each vessel was measured four to five times, and the measurements were averaged. Vessels <25 μm were excluded from further analysis. Calculations included blood velocity (μm/s): $(V_b) = V_v/2-[(D_s/D_v)^2]$, where D_s is the diameter of the microspheres (0.52 μm); volumetric blood flow (μm^3/s): $(Q) = V_b \times 0.625\ (CF) \times A_v]$; wall shear rate (s^{-1}): $(V_b \times 5\ (CF)/D_v] \times 2.13$; total leukocyte flux: (leukocytes) × Q; and rolling flux fraction: number of rolling leukocytes/total leukocyte flux.

Laser Injury Thrombosis Model. Thrombus formation was monitored using the laser-induced injury model as previously described (4, 5). Briefly, Dylight647-labeled antiplatelet (CD42b; 0.1 mg/g body weight) antibodies and Dylight488-labeled antifibrin (59D8; 0.5 mg/g body weight) antibodies were infused through a jugular vein catheter before injury. Cremaster arterioles were injured using a Micropoint Laser system (Photonics Instruments). Data were acquired digitally in two channels, 488/520 nm and 640/670 nm, prior and subsequent to a single laser injury. Images were captured using a CCD camera (Hamamatsu) for 180 s with an exposure of 0.5 frames/s. Data were analyzed using Slidebook 6.0 (Intelligent Imaging Innovations). For each thrombus, a mask was defined in the vessel upstream of the forming thrombus. The maximum fluorescent intensities of the pixels contained in the mask were extracted from all frames (pre- and postinjury). The mean value calculated from the maximal intensity values in the mask for each frame was determined and used as the background value. Calculations of background were made independently for each fluorescent channel. Finally, for each frame the integrated fluorescence intensity was calculated as per the following equation: Integrated fluorescence intensity = Sum Intensity of signal − (mean of the maximal background intensity × area of the signal). This calculation was performed for all frames in each thrombus and plotted versus time to provide the kinetics of thrombus formation. The data from 30 to 40 thrombi were used to determine the median value of the integrated fluorescence intensity to account for the variability of thrombus formation at any given set of experimental conditions.

Immunofluorescence. Cells were grown on glass coverslips in a 24-well culture plate to desired density. Following fixation by 4% paraformaldehyde (PFA) in PBS, cells were permeabilized (0.5% Triton-X100 in PBS) and blocked using immunofluorescence (IF) buffer (PBS containing 10% normal goat serum and 1% BSA) at 4 °C until staining or a minimum of 1 h at room temperature. Cells were incubated at room temperature for 1 h with the indicated primary antibodies, followed by appropriate AlexaFluor-488 or -555–conjugated secondary antibodies (ThermoFisher Scientific). Labeled cells were counterstained with nuclear dye, DAPI (ThermoFisher Scientific), or DRAQ5 (1:1,000, Cell Signaling Technologies) as suggested by the manufacturer. Coverslips were mounted onto glass slides using Aqua-Poly/Mount (Polysciences) and cured overnight before imaging. Visualization was completed utilizing a Zeiss LSM 810 Meta confocal scanning laser microscope. Fluorescent images of three colors were captured by sequentially using laser lines at 488, 561, and 633 nm to prevent spectral overlap of signals. Confocal micrographs were captured using Zeiss Zen Black software and exported as TIF files. Image analysis was completed utilizing the Fiji distribution package of ImageJ (6). Total fluorescent measurements were calculated for each channel (pAKT and AKT) of micrographs containing 40–50 nucleated cells per micrograph. The fluorescent intensity of pAKT and total AKT was reported as a ratio of pAKT to AKT.

Immunoblot Analysis. Following treatment, cells were lysed using either RIPA buffer with protease and phosphatase inhibitor mixture or Cell Signaling lysis buffer (for phosphoproteins) according to the manufacturer's instructions (ThermoFisher Scientific). Supernatants were diluted with reducing Laemmli buffer, and proteins were separated by SDS/PAGE. Subsequently, proteins were transferred and immunoblotted using specific primary antibodies and HRP-labeled secondary antibodies (Jackson ImmunoResearch Laboratories). Visualization of blots was completed by chemiluminescence using Supersignal West Pico Chemiluminescent substrate (ThermoFisher Scientific) or Optiblot (Abcam). Image capture and analysis was performed using the LAS-3000 Imager (Fujifilm Life Science) and analyzed using Image Quant TL software. Actin or GAPDH were utilized as a loading control.

Yo-Pro Apoptosis Assay. HUVECs were grown to confluence on glass coverslips in a 24-well cell culture plate and treated for 4 h with the indicated concentrations of parmodulin 1, parmodulin 2, or APC before treatment with vehicle, TNF (10 ng/mL), thrombin (1 unit/mL), or staurosporine (10 μM). Detection of apoptotic endothelial cells was evaluated using a modified version of the Vybrant apoptosis kit #4 (ThermoFisher Scientific) as previously described (3).

Caspase Assay. HUVECs were seeded in black, clear-bottom 96-well plates and grown until a confluent monolayer was formed. Cells were treated for 4 h with indicated concentrations of parmodulin 1, parmodulin 2, or APC followed by treatment with TNF (50 ng/mL) for 4 h. Following treatment, cells were fixed in the plate with 4% PFA for 15 min at RT. Cells were washed and permeabilized with 0.5% Triton X-100 in PBS for 5 min and blocked using IF buffer at 4 °C overnight. Cells were stained overnight at 4 °C with cleaved caspase-3 antibody (1/200 dilution) followed by incubation using an anti-rabbit Alexa 488-labeled secondary antibody (1/500 dilution). Cleaved caspase activity was measured using a SpectraMAX fluorescent plate reader (excitation at 485 nm and emission at 530 nm, cut off at 535 nm).

Factor Va Generation Assay. This assay was based on the factor Va activity assay described by Oliver et al. (7) with minor modifications. Confluent HUVECs were washed three times with HBS buffer (containing 1 mg/mL BSA and 3 mM $CaCl_2$) and subsequently incubated with 2 nM factor Va and 100 nM protein S in the presence or absence of APC (10 nM). Following a 15-min incubation, a solution containing 2.68 nM factor Xa, 2,800 nM prothrombin, and 600 μM chromogenic factor IIa substrate [CS-01(38), Biophen] was added to the cells to obtain a final concentration of 1.34 nM factor Xa, 1,400 nM prothrombin, and 300 μM of substrate. Absorbance at 405 nm was measured every 15 s for a total of 15 min.

1. Dowal L, et al. (2011) Identification of an antithrombotic allosteric modulator that acts through helix 8 of PAR1. *Proc Natl Acad Sci USA* 108:2951–2956.
2. Jasuja R, et al. (2012) Protein disulfide isomerase inhibitors constitute a new class of antithrombotic agents. *J Clin Invest* 122:2104–2113.
3. Aisiku O, et al. (2015) Parmodulins inhibit thrombus formation without inducing endothelial injury caused by vorapaxar. *Blood* 125:1976–1985.
4. Falati S, Gross P, Merrill-Skoloff G, Furie BC, Furie B (2002) Real-time in vivo imaging of platelets, tissue factor and fibrin during arterial thrombus formation in the mouse. *Nat Med* 8:1175–1181.
5. Jasuja R, et al. (2012) Protein disulfide isomerase inhibitors constitute a new class of antithrombotic agents. *J Clin Invest* 122:2104–2113.
6. Schindelin J, et al. (2012) Fiji: An open-source platform for biological-image analysis. *Nat Methods* 9:676–682.
7. Oliver JA, Monroe DM, Church FC, Roberts HR, Hoffman M (2002) Activated protein C cleaves factor Va more efficiently on endothelium than on platelet surfaces. *Blood* 100:539–546.

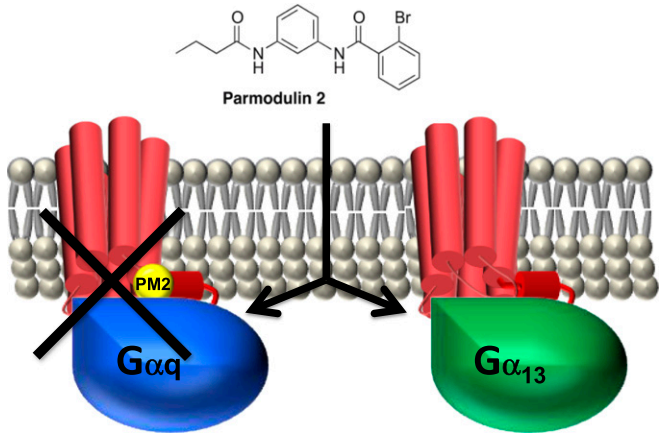

Fig. S1. Parmodulins exhibit biased signaling. Previous studies have demonstrated that parmodulins (e.g., PM2 shown in yellow) act at the cytosolic face of PAR1 (red). Parmodulins demonstrate biased antagonism, inhibiting signaling mediated by Gαq (blue), but not by $G\alpha_{13}$ (green).

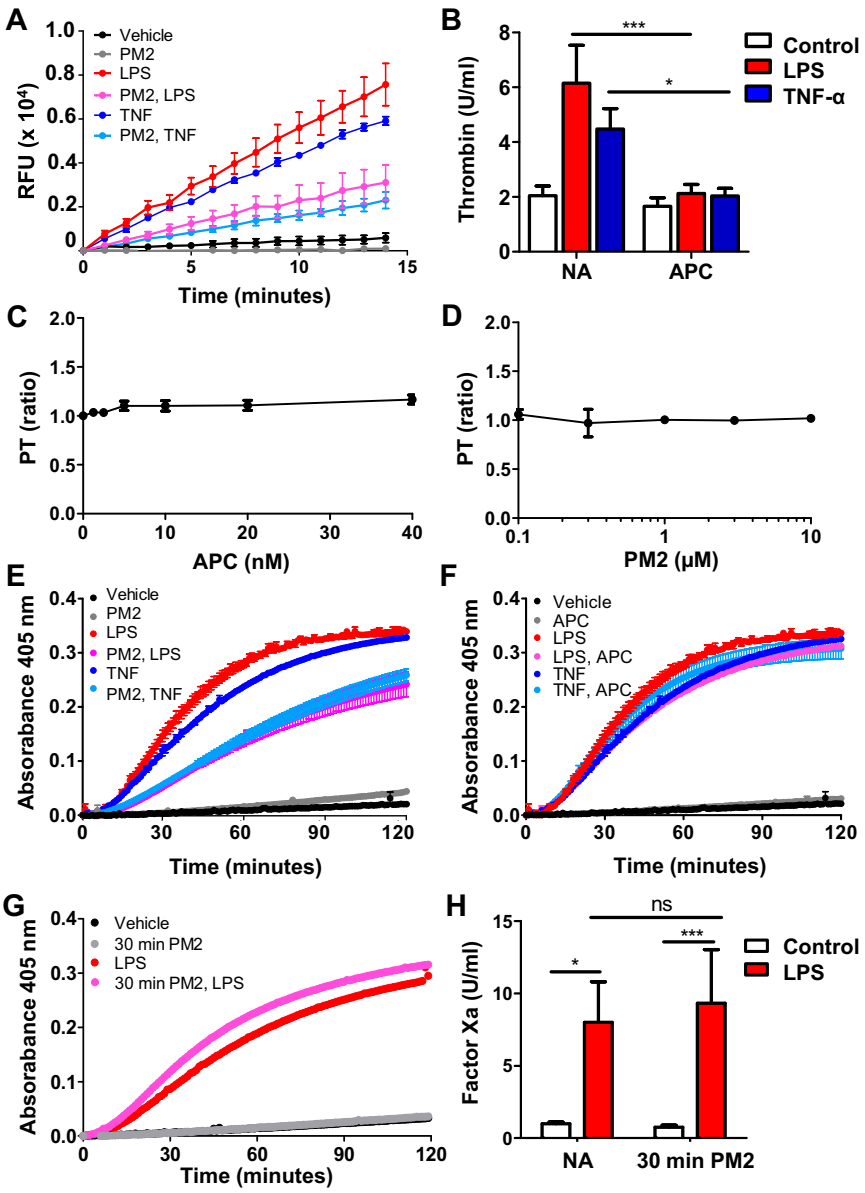

Fig. S2. Parmodulin 2 blocks inflammation-induced thrombin and factor Xa generation upon prolonged exposure. (*A*) HUVECs were preincubated with vehicle or PM2 (3 μM) for 4 h. Samples were either left untreated (vehicle) or then exposed to TNF-α (10 ng/mL) or LPS mixture (100 ng/mL LPS, 10 ng/mL LBP, 100 ng/mL sCD14) for an additional 4 and 3 h, respectively. Thrombin generation was monitored using the fluorogenic substrate SN-20. (*B*) HUVECs were exposed to TNF-α (10 ng/mL) or LPS mixture for 4 and 3 h in the presence or absence of APC (10 nM). Thrombin generation was monitored using a fluorogenic thrombin substrate. Values were normalized to controls and are depicted as mean ± SEM ($n \geq 5$). One-way ANOVA with Bonferroni posttests was used to compare groups. $^{*}P < 0.05$; $^{***}P < 0.001$. Comparison of the dose dependency of (*C*) APC and (*D*) PM2 in a PT assay. Clotting times are represented as the ratio of samples containing APC or PM2 versus control samples. Data represent mean ± SEM of three samples normalized to control samples. HUVECs were pre-incubated with (*E*) vehicle versus PM2 (3 μM) or (*F*) vehicle versus APC (10 nM) for 4 h. Samples were either left untreated (vehicle) or subsequently exposed to TNF-α (10 ng/mL) or LPS mixture for an additional 4 and 3 h, respectively. Factor Xa generation was monitored using a chromogenic FXa substrate. Absorbance at 405 nm was measured and depicted as a function of time. (*G* and *H*) HUVECs were treated with vehicle or PM2 (3 μM) for 30 min followed by treatment with LPS mixture for an additional 3 h. Factor Xa generation was measured using a chromogenic FXa substrate. Absorbance at 405 nm was measured and depicted as a function of time. (*H*) Values are normalized to controls and depicted as mean ± SEM ($n = 9$). The Kruskal–Wallis test was used to compare groups. $^{*}P < 0.05$; $^{***}P < 0.001$. ns, nonsignificant.

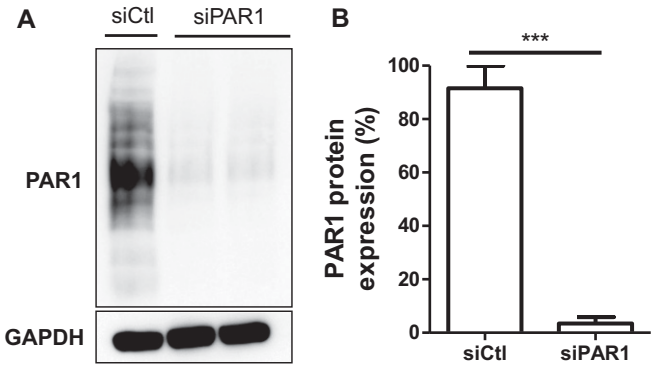

Fig. S3. Confirmation of PAR1 knockdown. HUVECs were transfected with control siRNA (siCtl) or PAR1 siRNA (siPAR1). Following a 48-h incubation, cell lysates were prepared and blotted for PAR1 and GAPDH (loading control). (*A*) Representative experiment. (*B*) Quantification of immunoblot analysis. PAR1 protein expression was determined by measuring the ratio of PAR1 versus GAPDH and depicted relative to control siRNA-treated cells (siCtl; set as 100%). Student *t* test ($n = 3$) was used for statistical significance. ***$P < 0.001$.

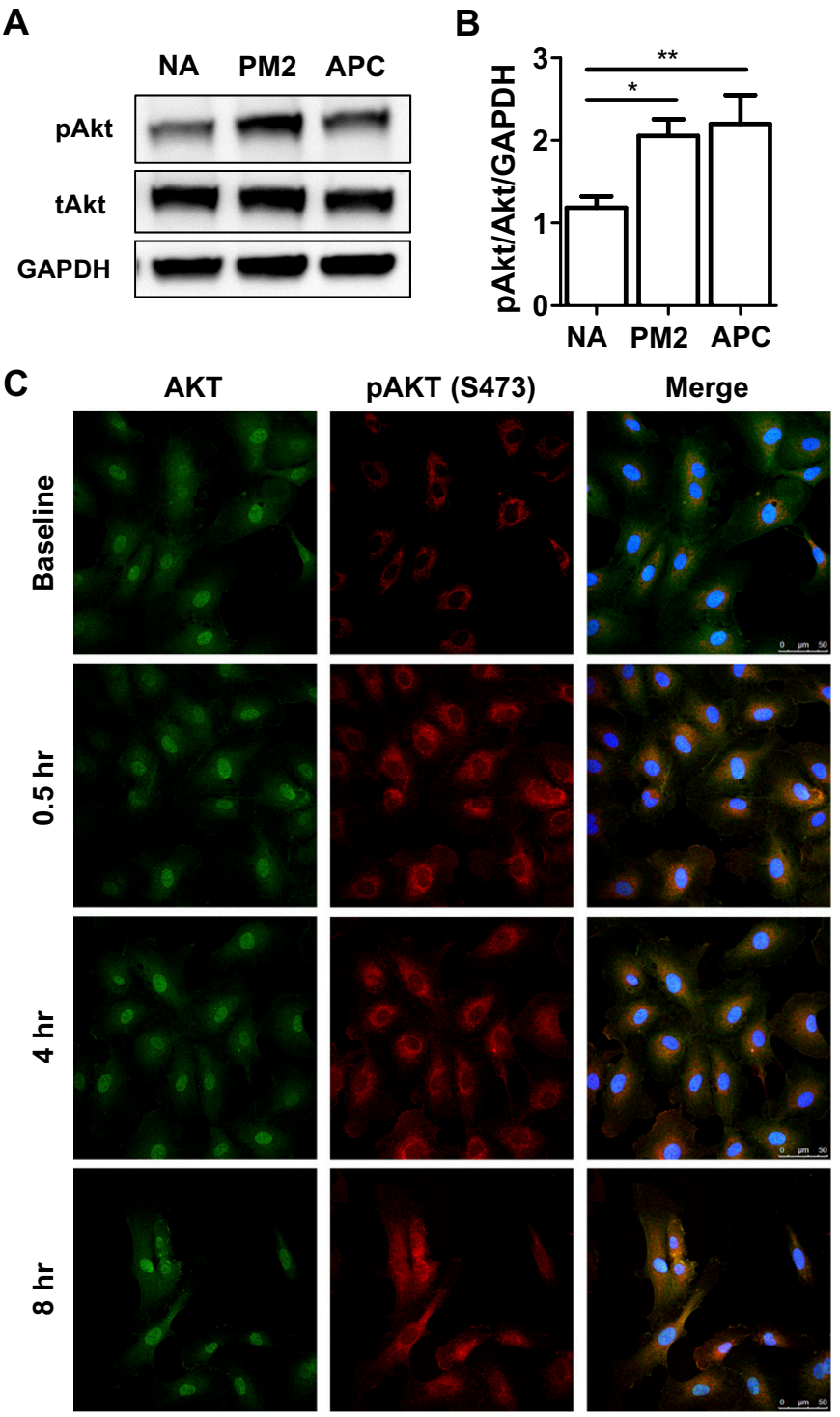

Fig. S4. Parmodulin 2 induces Akt phosphorylation. (*A* and *B*) HUVECs were incubated with vehicle, 10 μM PM2, or 10 nM APC for 15 min. Cell lysates were immunoblotted for pAkt (Ser473), total Akt, and GAPDH (loading control). Representative image (*A*) and quantification (*B*) of the effect of PM2 and APC on pAkt. Data represent mean ± SEM ($n \geq 5$). One-way ANOVA with Bonferroni posttests was used to compare groups. *$P < 0.05$; **$P < 0.01$. (*C*) Time course of Akt phosphorylation. HUVECs were exposed to either vehicle or 3 μM PM2 for 0.5, 4, or 8 h. Samples were then stained using an anti-Akt antibody (green), anti–phospho-Akt (Ser473) antibody (red), and DRAQ5 (blue). Samples were evaluated using three-color confocal immunofluorescence microscopy. (Scale bar: 50 μm.)

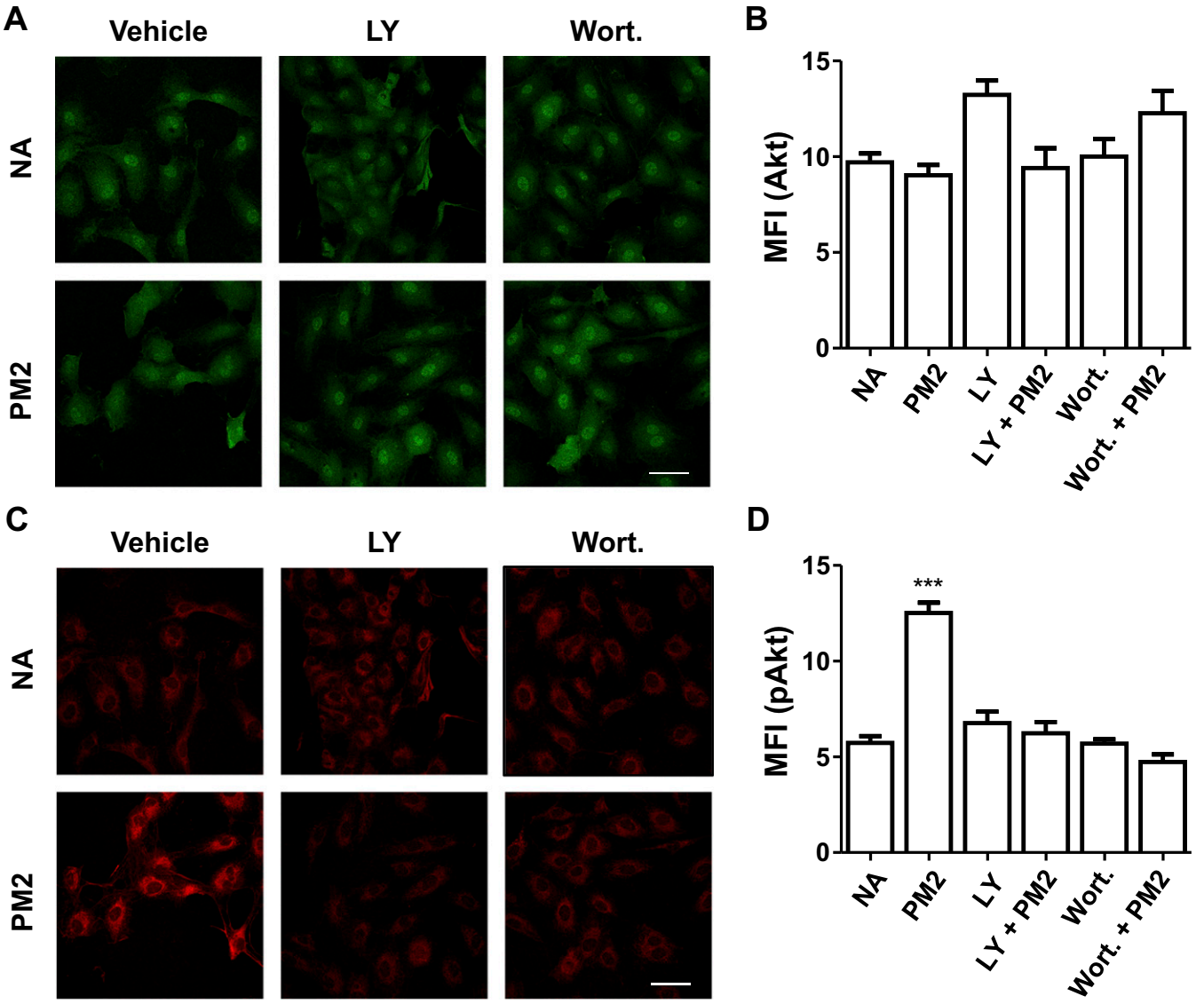

Fig. S5. Parmodulin 2 stimulates Akt via a PI3-kinase–dependent pathway. HUVECs were incubated with either vehicle (NA), 0.1 μM wortmannin (wort), or 50 μM LY294002 (LY) and subsequently exposed to either vehicle or PM2 (3 μM) as indicated. Samples were analyzed for (*A* and *B*) total Akt or (*C* and *D*) phospho-Akt using confocal immunofluorescence microscopy, and staining intensity was quantified using Image J. (Scale bars: 50 μm.) Data represent mean ± SEM ($n = 5$). One-way ANOVA with Bonferroni posttests was used to compare groups. ***$P < 0.001$.

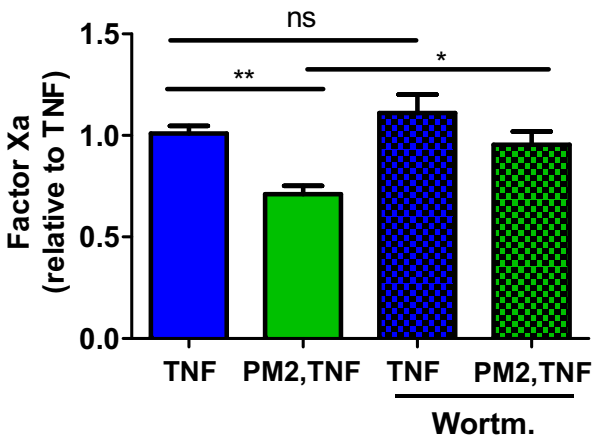

Fig. S6. The protective effect of parmodulin 2 is PI3K-dependent. HUVECs were preincubated with vehicle or PM2 (10 μM) for 4 h in the absence or presence of wortmannin (Wortm.; 0.1 μM). Samples were then exposed to TNF-α (10 ng/mL) for an additional 4 h ± wortmannin (Wortm.; 0.1 μM). Factor Xa generation was monitored using a chromogenic factor Xa substrate. Values were normalized to TNF samples and are depicted as mean ± SEM ($n = 6$). One-way ANOVA with Bonferroni posttests was used to compare groups. *$P < 0.05$; ** $P < 0.01$. ns, nonsignificant.

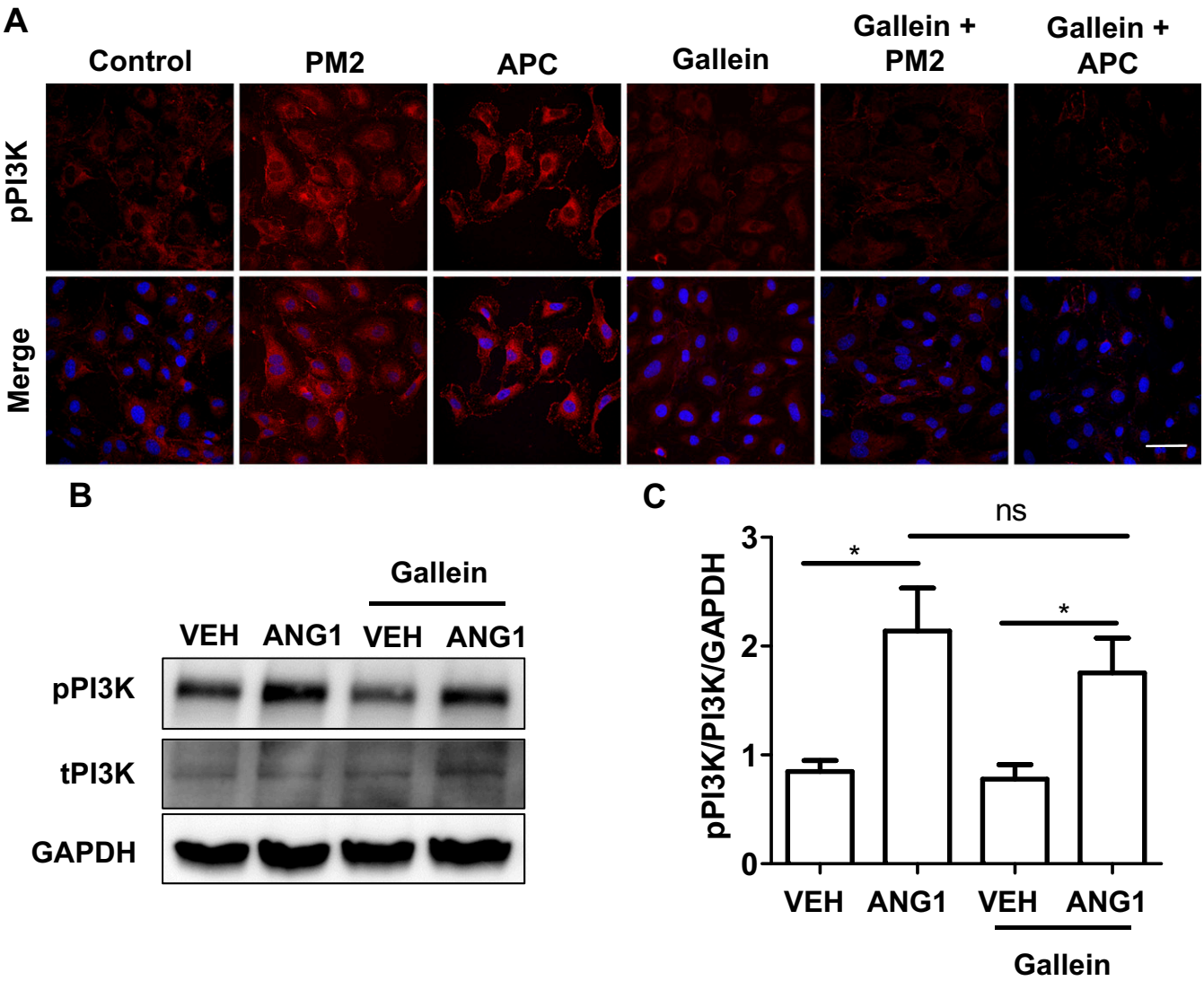

Fig. S7. Activation of PI3-kinase by parmodulins and APC is mediated by Gβγ. (*A*) HUVECs were incubated in the presence or absence of 60 μM gallein for 30 min. Samples were subsequently exposed to either vehicle (NA), PM2, or APC for 4 h and stained using an a phospho-PI3K antibody (red) and DRAQ5 to visualize nuclei (blue). Samples were then evaluated using confocal immunofluorescence microscopy. (Scale bar: 50 μm.) (*B* and *C*) HUVECs were incubated in the presence or absence of 60 μM gallein for 30 min followed by incubation with angiopoietin-1 (ANG1; 200 ng/mL) for an additional 4 h. (*B*) Representative immunoblot of cell lysates stained for pPI3K and tPI3K. GAPDH was used as a loading control. (*C*) Quantification of immunoblot analysis. Values are represented relative to vehicle-treated cells. Data represent mean ± SEM ($n = 7$). One-way ANOVA with Bonferroni posttests was used to compare groups. *$P < 0.05$. ns, nonsignificant.

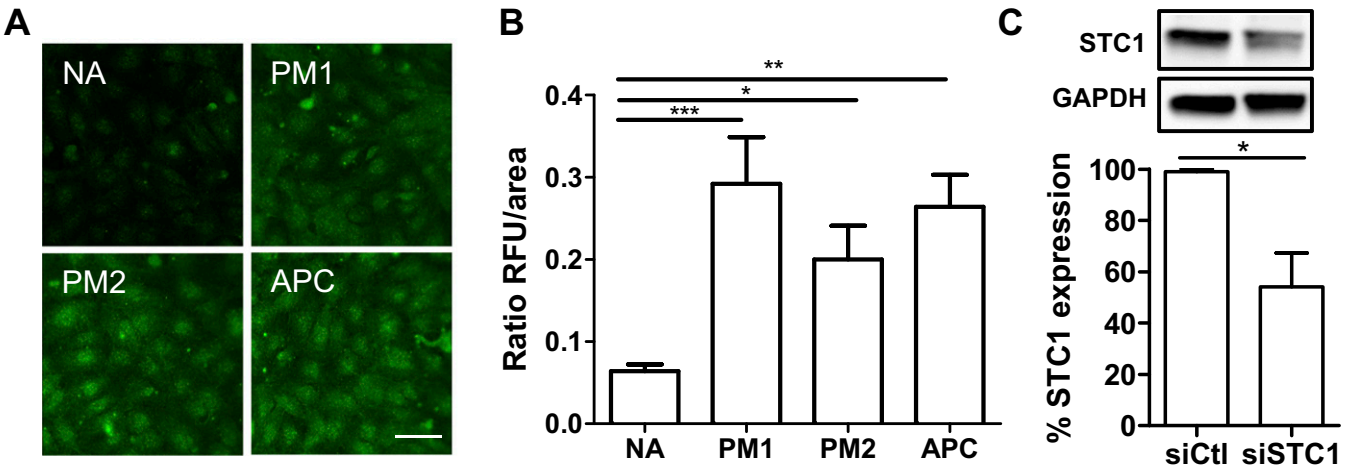

Fig. S8. Stanniocalcin 1 is up-regulated by parmodulins or APC in endothelium. (*A* and *B*) Following incubation for 4 h with vehicle, PM1 (10 μM), PM2 (3 μM), or APC (10 μg/mL), HUVECs were stained with anti-STC1 antibody and evaluated by immunofluorescence microscopy. (*A*) Representative images. (Scale bar: 50 μm.) (*B*) Data indicate the mean ± SEM ($n = 5$). One-way ANOVA with Bonferroni posttests was used to compare PM1, PM2, and APC to control (NA). *$P <$ 0.05; **$P < 0.01$; ***$P < 0.001$. (*C*) Confirmation of STC1 knockdown by immunoblot. HUVECs were transfected with control siRNA (siCtl) or STC1 siRNA (siSTC1). Following a 48-h incubation, cells were serum-starved for 1 h and then incubated in basal media containing 50 ng/mL VEGF. Cell lysates were prepared and blotted for STC1 and GAPDH (loading control). Quantification of immunoblot analysis was performed using Image Quant TL software. STC1 protein expression was determined by measuring the ratio of STC1 versus GAPDH and depicted relative to control siRNA-treated cells (siCtl; set as 100%). Student *t* test ($n = 4$–6) was used for statistical significance. *$P < 0.05$. (*Inset*) Representative experiment.

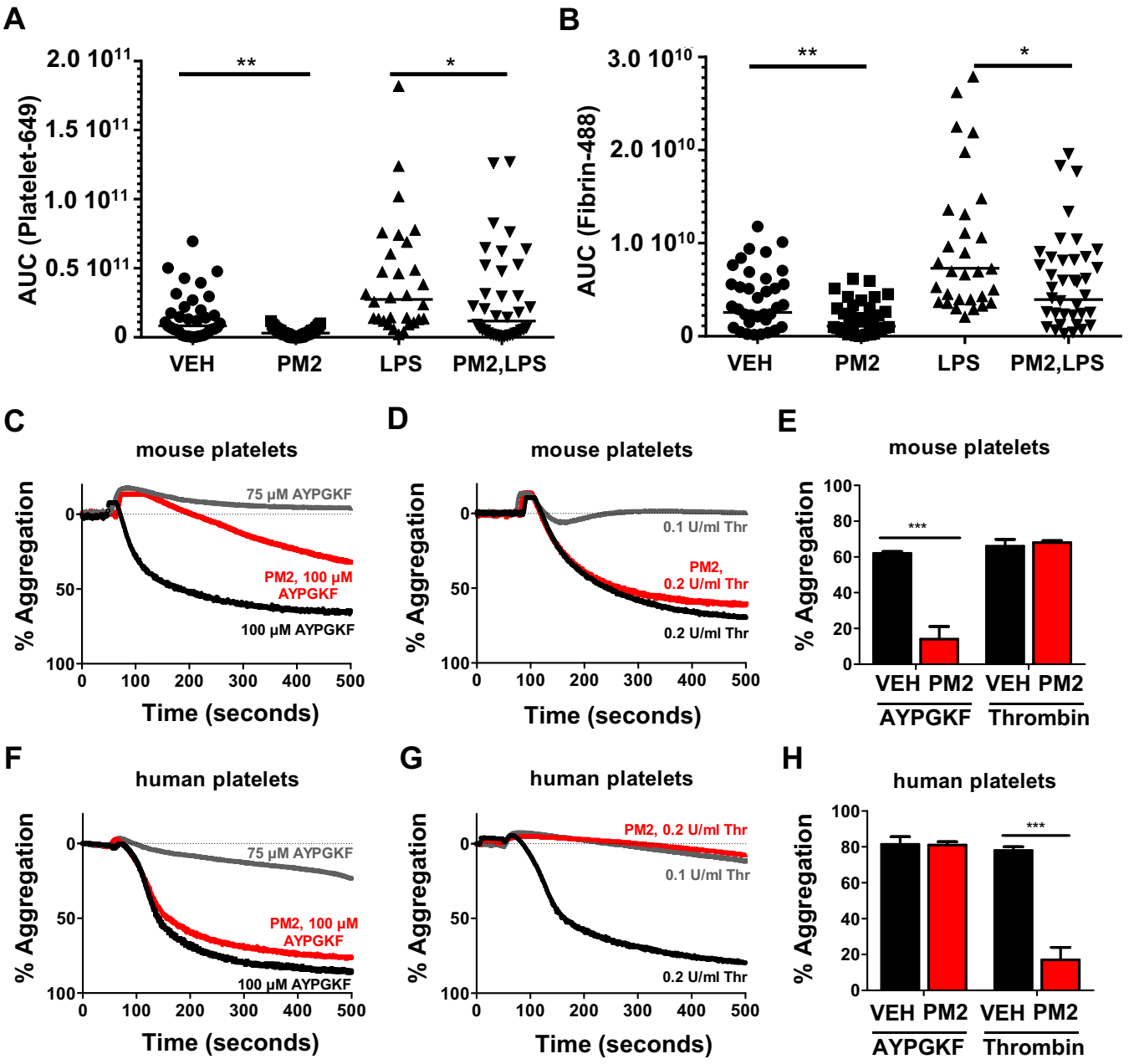

Fig. S9. Parmodulin 2 inhibits LPS-enhanced thrombus formation in vivo by acting on the endothelium. (*A* and *B*) Mice ($n = 3–4$ per experiment) were injected with vehicle or PM2 (5–10 mg/kg) 2.5 h before 10 mg/kg LPS administration (IP) and an additional bolus injection 0.5 h after LPS exposure. Thrombus formation was induced by endothelial laser injury in cremaster arterioles 1–3 h following LPS injection. Platelet and fibrin accumulation were monitored for 180 s using Dylight 647-labeled antiplatelet antibody (CD42b) and Dylight 488-labeled antifibrin antibody (59D8). Area under the curve (AUC) for platelet (*A*) and fibrin (*B*) fluorescent intensities was calculated for all individual thrombi in vehicle ($n = 37$), PM2 ($n = 37$), LPS ($n = 30$), and PM2 followed by LPS ($n = 38$) experiments. A Kruskal–Wallis test with multiple comparisons was used. $^{*}P < 0.05$, $^{**}P < 0.01$. To evaluate whether the inhibition of thrombus formation by PM2 in this model was primarily owing to its antiplatelet or its cytoprotective effect, we evaluated the ability of PM2 to block thrombin-induced platelet aggregation. Mouse (*C*–*E*) and human (*F* and *G*) washed platelets were incubated with vehicle or 5 μM PM2 for 30 min before addition of PAR4-agonist or thrombin. (*C* and *F*) Platelet aggregation in response to 75 μM AYPGKF (gray) or 100 μM AYPGKF (gray and black) was monitored. These results were consistent with our previous finding that parmodulins block mouse PAR4, which has a cysteine palmitoylation site at the C-terminal of its eighth helix (1), but not human PAR4, which lacks a palmitoylation site. (*D* and *G*) Evaluation of platelet aggregation in response to 0.1 U/mL thrombin (dark gray) and 0.2 U/mL thrombin (light gray and black) showed that thrombin overcomes PM2-mediated inhibition of mouse platelet aggregation, but not its ability to block human platelet aggregation to low-dose thrombin. (*E* and *H*) Quantification of aggregation in response to 100 μM AYPGKF and 0.2 U/mL thrombin. Data represent mean ± SEM ($n = 3–6$). One-way ANOVA with Bonferroni posttest was used to compare groups. $^{***}P < 0.001$.

1. Dowal L, et al. (2011) Identification of an antithrombotic allosteric modulator that acts through helix 8 of PAR1. *Proc Natl Acad Sci USA* 108:2951–2956.

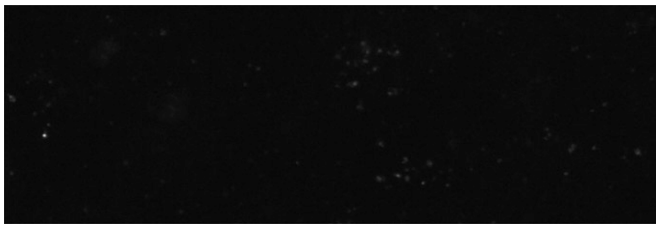

Movie S1. Bioengineered microvessels exposed to vehicle alone (corresponding to Fig. 1*F*, vehicle). A composite video made from separate videos of an endothelial cell surface is shown. Separate fields have been spliced together to create the video.

Movie S1

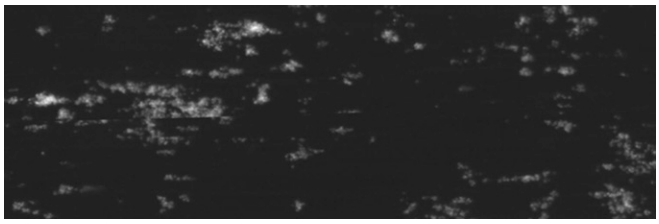

Movie S2. Bioengineered microvessels exposed to TNF (corresponding to Fig. 1*F*, TNF-α). A composite video made from separate videos of an endothelial cell surface is shown. Separate fields have been spliced together to create the video.

Movie S2

Movie S3. Bioengineered microvessels exposed to PM2 alone (corresponding to Fig. 1*F*, PM2). A composite video made from separate videos of an endothelial cell surface is shown. Separate fields have been spliced together to create the video.

Movie S3

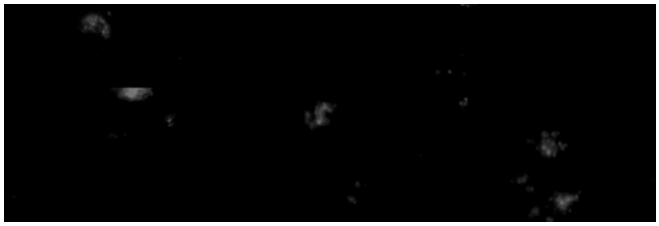

Movie S4. Bioengineered microvessels exposed to PM2, TNF (corresponding to Fig. 1*F*, PM2, TNF-α). A composite video made from separate videos of an endothelial cell surface is shown. Separate fields have been spliced together to create the video.

Movie S4